Indian Journal of Engineering & Materials Sciences
Vol. 29, April 2022, pp. 228-236

Effect of input variable of GMAW on microstructure and mechanical properties of High Strength Low Alloy

Saurabh Kumar Gupta[a], Rajnish Singh[b], & Saadat Ali Rizvi[c*]

[a]Carriage and Wagon, North-Eastern Railway, Gorakhpur, Uttar Pradesh 273 012, India
[b]Department of Mechanical Engineering, Kamla Nehru Institute of Technology, Sultanpur, Uttar Pradesh 228 118, India
[c]University Polytechnic, Jamia Millia Islamia, New Delhi 110 025, India

Received: 16 February, 2021; Accepted: 30 December, 2021

The present study focused on evaluating mechanical and microstructural properties of Gas Metal Arc (GMA) welded High Strength Low Alloys (HSLA) steel weldments at different heat inputs. Heat input plays a significant role in influencing welded joints' mechanical properties and microstructure. Nine different values of heat input were considered and the range of heat input value was from 1.89-2.61Kj/mm. From the results it was found that on increasing the heat input in the form of input parameters, the average Ultimate Tensile Strength (UTS) was increased and then decreased but at the same time grain coarsening in microstructure was also observed. From the rest result, it was also observed that on increasing the heat input value toughness of weldment also increases.

Keywords: High Strength Low Alloys (HSLA), Scanning Electron Microscope (SEM), Ultimate Tensile Strength (UTS), Heat Affected Zone (HAZ), Microstructure, Heat input

1 Introduction

The fabrication of High-Strength Low Alloys (HSLA) alloys is prominent in railways because most of the bodies of the railways are made of HSLA alloys. Therefore fabrication comes into the picture. The automobile industries are also using the HSLA alloys tremendously. The low-cost and high-strength alloys are favoured by automobile and submarine industries. Excellent weldability is the key feature of HSLA alloys. The weldability will depend upon the input variable as well as the welded design. The effect of heat input in the GMA welding process of stainless steel develops martensite and toughness of metal after welding[1]. The development of martensite in the microstructure improves the fracture strength of the metal. The welding of HSLA alloy is still challenging due to its hot cracking tendency along the centerline. Its major source of failure of HSLA. The centerline cracking is initiated during the solidification of the weld. The solidification crack was induced due to the high depth of weld and slow welding speed and improper weld design. In the case of microstructure evaluation of centre, line cracking is due to low melting point constituent in the workpiece[2]. The low melting point constituent develops a large range of solidification. Such problems can be reduced with the use of proper input parameters so that solidification can be made possible in proper order. The hot and cold cracking of HSLA alloy can be improved by changing the combination of elements in alloys such as Mn, Ni, Ti, Cr, and Mo. The Ni can improve the volume fraction of acicular ferrite in the alloys HSLA. A similar effect can also be reported by other authors with Cr. The combination of Ni, and Cr and their ratio is also used for improvement in the cold and hot cracking. But Ni can also influence the microstructure of HSLA steel[3]. Therefore the changing of microconstituents and composition produced another microstructural problem in HSLA. So that the input variable such as heat input was taken as the event that can improve the mechanical and microstructural properties of HSLA[4]. The effect of heat input on mechanical properties was investigated with nine different experiments on GMA welding of HSLA. The microstructural characterization of laser beam welded steel of niobium alloys is also quite similar to HSLA alloys and the effect of laser power put a similar effect as in the case of GMAW[5-6]. The effect of heat input on underwater welding was also studied and found to improve the tendency of cracking and improve the microstructure and mechanical properties of HSLA in flux-cored arc welding[7]. The effect of

*Corresponding author (E-mail:sarizvi1@jmi.ac.in)

heat input in the case of multipass was also analyzed and found to be less heat input required for better strength in the second pass of the bead. The multi-pass welding was studied in the HSLA alloy for Metal Inert Gas (MIG) welding[8]. The bead geometry, strength, and heat input relation were established with the use of regression analysis. An analysis of weld bead geometry was predicted by an Artificial Neural Network (ANN) in the TIG welding process on HSLA[9]. A hot wire gas tungsten welding was done on HSLA and studied the heat input on HSLA[10]. The optimization technique can also be used for the prediction of the mechanical properties of the welded part. The optimization of process parameters was used for optimizing the heat input condition in FSW welding[11]. The effect of heat input becomes a prime function for microstructure in the case of electron beam welding. The density of heat input in the case of electron beam welding is very high as compared to GMA welding[12]. The friction of heat input can be used for friction stir welding. The microstructure evaluation is different as in the case of the fusion welding process[13]. Rizvi S A[14] studied the effect of heat input on mechanical properties and microstructure of AISI 304 steel weldments by GMA welding and the author informed that on increasing the heat input value ultimate tensile strength (UTS) of weldments decreases. Jorge J C F *et al*[15] reviewed microstructure characterization and its relation with the toughness of HSLA steel weldments and they informed that acicular is not the main constituent that always affects the toughness.

2 Materials and Methods

2.1 Material

In this research work, HSLA steel was used as a base material. A 10 mm thick plate of HSLA was welded by the GMAW process. The welded design also plays a significant role in the development of mechanical and microstructural properties of the welded joint, V groove was selected for weld bead. To ensure the full penetration, the multiple pass weld was performed along the weld centerline. The welding current and voltage was prime input variable of GMA welding. The range of current was available 100-400 A and voltage was in the range of 15- 40 V. A weld joint was prepared by Ø 1.2 mm filler rod and the filler rod material was the same material as the base material. The wire feed rate can also be moderate depending upon the requirement. CO_2 gas was used for shielding purposes during the welding process in the current study. The chemical composition of base metal (HSLA), filler wire, and mechanical properties are tabulated in Table 1 and Table 2 respectively.

V-groove and experimental setup used in the present study are shown in Fig. 1(a and b) respectively. ASTM A242 type-II standard was used to fabricate the tensile test samples. total nine tensile test samples at different heat inputs are shown in Fig. 1(c)

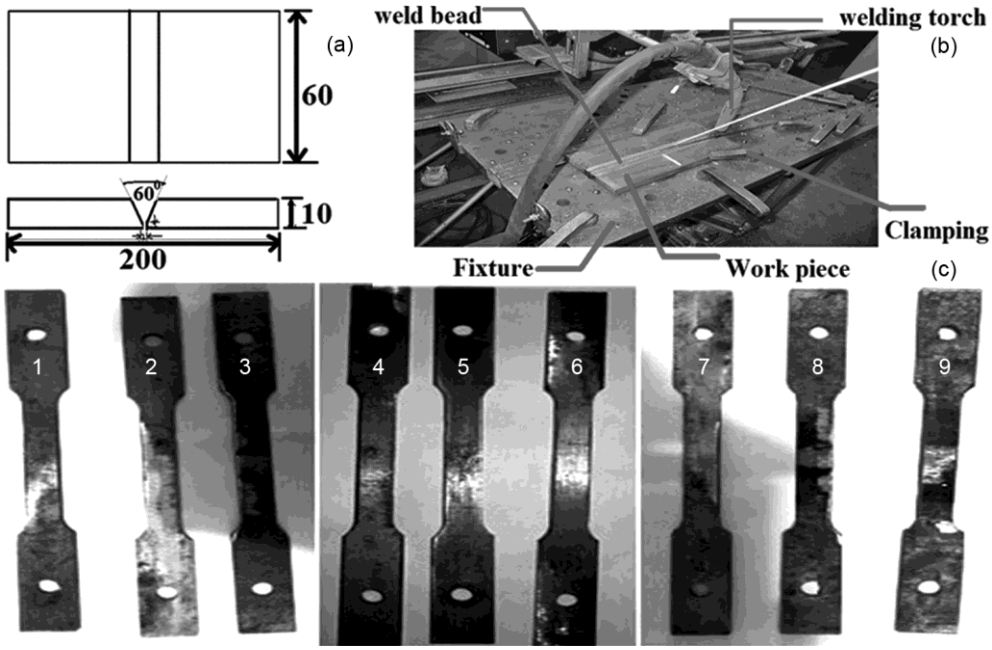

Fig.1 — (a) V-groove detail of sample (all dimensions in mm), (b) actual welding setup, and (c) tensile test samples.

Table 1 — Chemical composition of the parent metal and filler wire

Material	% of C	% of Cr	% of Ni	% of S	% of Mn	% of Cu	% of Si	Fe
HSLA	0.196	0.06	0.04	0.05	1.0056	0.029	0.5	Rest
Filler wire 308	0.035	18.5	8.55	0.04474	1.2647	0.137	---	

Table 2 — Mechanical properties of base metal

Material	YS (MPa)	UTS (MPa)	% Elongation	Toughness (J)	Hardness (HV)
HSLA	328	456	46	111	80

Table 3 — GMA welding process parameters

Weld Sample No	Welding current (A)	Arc voltage (V)	Heat input (Kj/mm)
1	128	17	1.89
2	140	20	1.93
3	150	23	2.01
4	185	26	2.1
5	200	29	2.19
6	210	32	2.29
7	225	35	2.4
8	240	38	2.5
9	250	41	2.61

Table 3 represents welding parameters selected for analysis of heat effect. The current in Ampere and voltage in volt are tabulated for different samples in Table 3

The welded joints prepared under the different heat input levels have different values of ultimate tensile strength, toughness, and Vickers hardness. Microstructures of weld zone also show a varying trend for different welding current, arc voltage, and welding speed combinations i.e. heat input. During the welding process shielding,the gas flow rate was 10 l/min.

3 Results and Discussion

3.1 Mechanical Properties

3.1.1 Effect of heat input on absorbed energy (toughness) of the weld zone

The Charpy or Izod test was performed to analyze the absorbed impact energy by the weld samples. The amount of absorbed energy depends upon the nature of the material after welding as if the weldment is ductile then the absorbed energy will be more. In the case of HSLA steel as the heat input increases the amount of energy absolved increases. This is due to coarsening of grains. The cause grain material can absorb more amount of energy. The coarsening of grains is the result of the slow cooling rate of weldments. Large heat input means less amount of voltage and current is more at the same time reduced feed rate also plays a role for coarsening of grain. The samples were prepared for the Charpy test as per

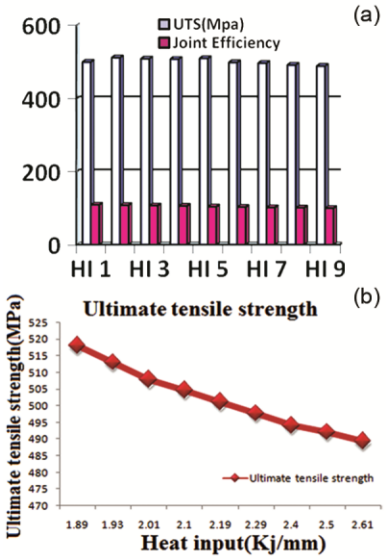

Fig. 2 — (a) Variation of absorbed energy with heat input (HI), and (b) toughness test samples after fracture.

ASTM standards,experiments were conducted and results are tabulated in Fig. 2(a). From Fig. 2(a) it is clear that on increasing the heat input value there is an increment in the toughness of weldment.

The Charpy test images are shown in Fig. 2(b). The cold cracking of HSLA steel was also evident in the Charpy test that almost all the fracture was found along the centerline.

3.1.2 Effect of heat input on tensile strength

The tensile test is the robust test method of mechanical properties evaluation The tensile test measure the relationship between load and elongation of the samples. The yield strength, ultimate tensile strength, fracture point, toughness, and resilience can be calculated by the tensile test. The three samples were prepared for each heat input condition testing and a total of 27 tensile test samples were performed and results are shown in Fig. 3(a). From previous research work, it is also clear that the mechanical properties of weldments are affected by the heat input value.

Figure 3(a) shows the combined effect of voltage, current and welding speed i.e. heat input on ultimate

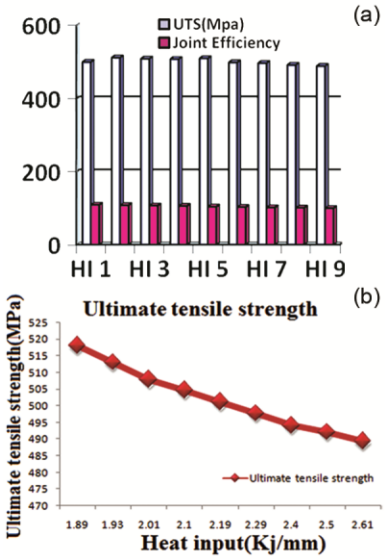

Fig. 3 — (a) Weld joint efficiency with welding parameters, and (b) variation of ultimate tensile strength with heat input.

tensile strength of weld zone. The curve shows a decreasing trend[16]. This was the indication of better tensile strength was found at low heat input conditions as shown in Fig. 3(b) which can attribute to smaller dendritic size with a small spacing infusion zone. Relatively lower tensile strength and ductility are possessed by the joints with long dendrite sizes and large inter-dendritic spacing in the fusion zone of the joint welded using high heat input. Further, it is observed that all the tensile test samples fractured from the base metal which represents that weldments possessed higher tensile strength than the parent metal i.e. HSLA steel.

3.2 SEM fractography of fractured surface of tensile test samples

SEM fractography of fractured tensile test samples is shown in Fig. 4. Ductilefractures were observed with varying sizes and shapes of dimples on all surfaces[17]. The fracture surface appeared as mixed mode[18], irrespective of heat input and temperature. The fracture mode analysis in the tensile sample found the ductile or brittle fracture analysis. During the tensile test, after yielding small microvoids are found then these voids start increasing their size in the elliptical form in ductile fracture. And the end of the test these voids were converted into two parts.These dimples can be seen in the SEM analysis. But in the case of brittle fracture, the microvoids were found but did not enlarge in elliptical shape thus such images were not found in the SEM images. Figure 4 found that more population of dimples in the SEM image had low heat input conditions. The SEM images of Fig. 4, samples 2 to 9 was showing corse and enlarges dimples that were increased heat input conditions.

3.4 Microhardness of weld zone (WZ)

The microhardness test was done with a diamond indentor for analysis of different zones found at the welding seam line. The hardness changes as we move from the weld centerline. The complete analysis was done in two different directions to analyze the heat-affected zone width and fusion zone area. Figure 5 Sample 2, 3, and 4 shows the variation of microhardness in the lateral and longitudinal directions. The cooling rate at the top surface was higher so it was found higher microhardness in all microhardness test results. The cooling rate reduces in the thickness direction, found reduced microhardness. The effect of heat input from minimum to maximum was found an adverse effect on hardness. Higher the heat input found lower hardness. As the heat input increases from a lower level to a higher level, the microhardness at the weld centre reduces rapidly. The formation of acicular ferrite[19] in the fusion zone develops high hardness. The microhardness at the boundary of the fusion zone produced a low hardness value that was evident at the start of the HAZ zone. The fusion zone was completely melted. At the boundary of the fusion, zone reduced hardness result that caused grains. The microhardness was at the base metal and the HAZ boundary abruptly increases. That was due to the fast heat transfer rate. This zone is found with a moderate cooling rate[20]. Therefore coarsening of grains found in this zone. Thus from all microhardness analyses, different was analysis on variable heat input conditions.

3.5 Microstructural examination

The micro store is the image of the top surface. The microstructural analysis was done for all samples at different heat input conditions as shown in Figs (6-11). The micrograph was taken for the fusion zone and HAZ zone for all samples as shown in Figs 10 and 11. The weld centerline found the columnar grain as shown in Fig. 10 and some fusion zone found the alleged dendrites and ferritic structure in the fusion zone as shown in Fig. 11 (a and b) at different zoom conditions. On increasing the heat input condition the acicular ferrite first increases then decreases. The size of acicular ferrite[21] depends upon the heat input also. Heat input increases the increased grain size and reduced hardness. As the heat input increases the interspacing of dendritic increases[22-23]

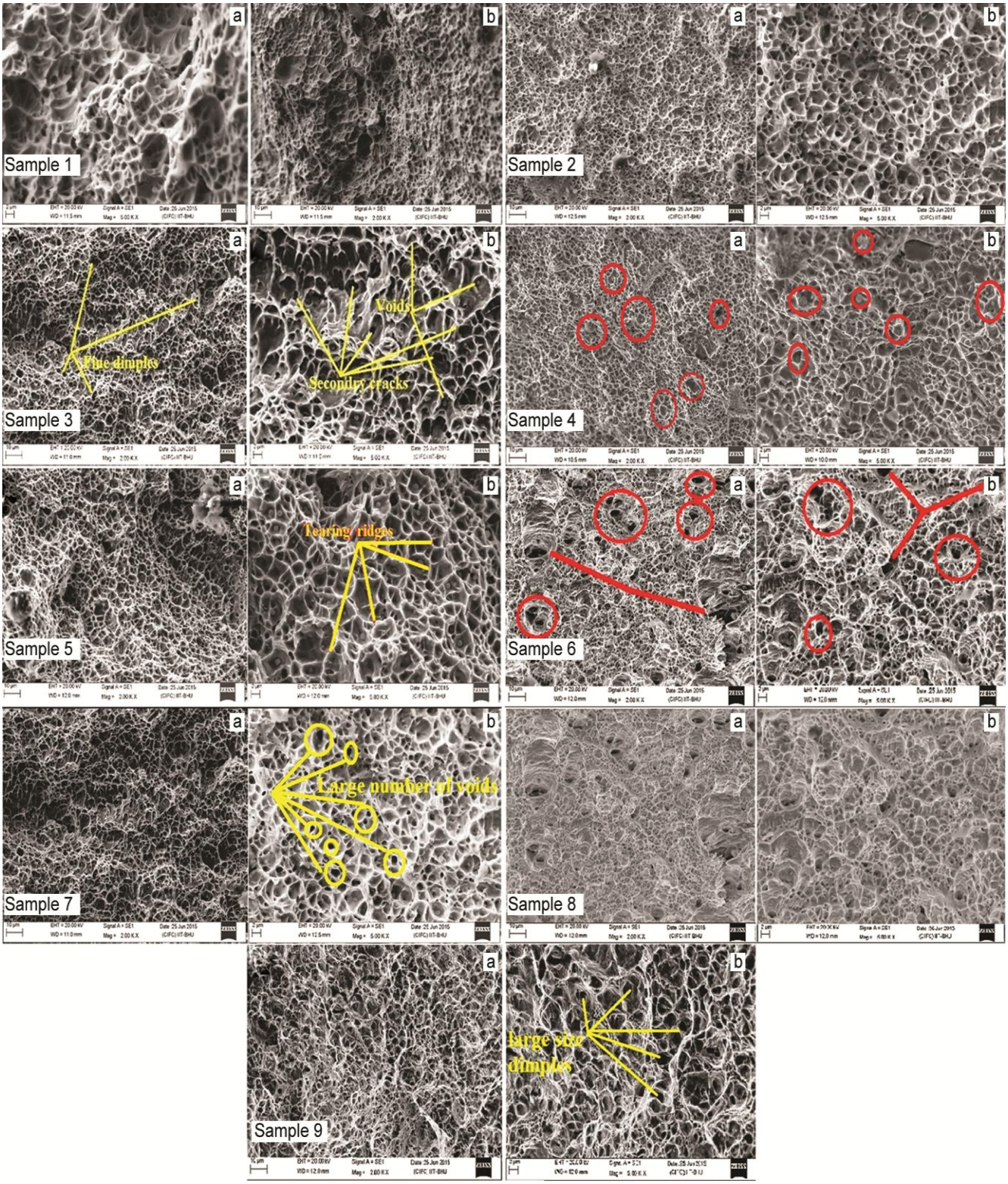

Fig. 4 — SEM fractography of the tensile sample no. 1 to sample no. 9 at 5000X.

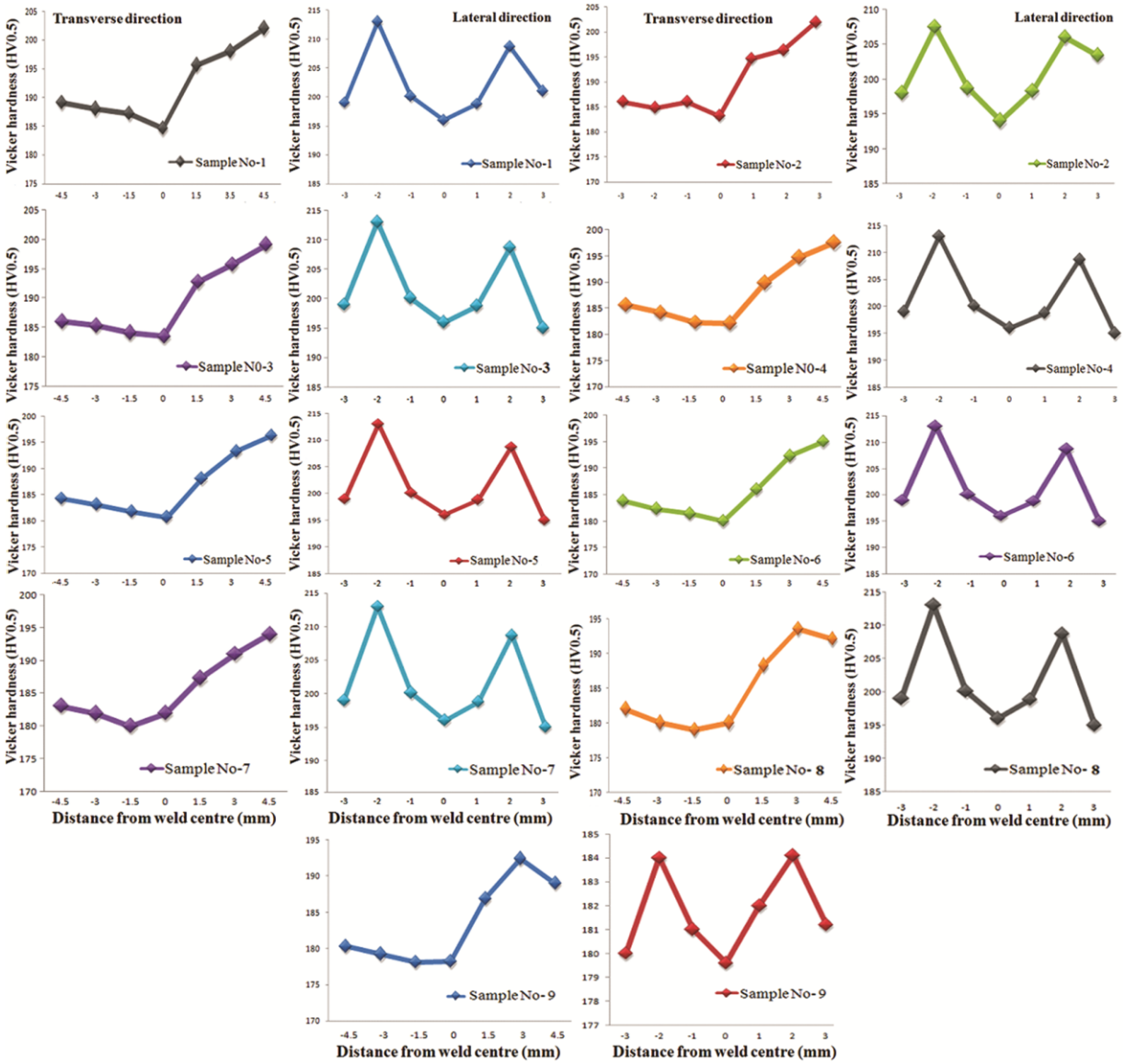

Fig. 5 — Microhardness distribution showing micro-hardness at different points in weld metal in the transverse and lateral direction of sample no. 1 to sample no. 9.

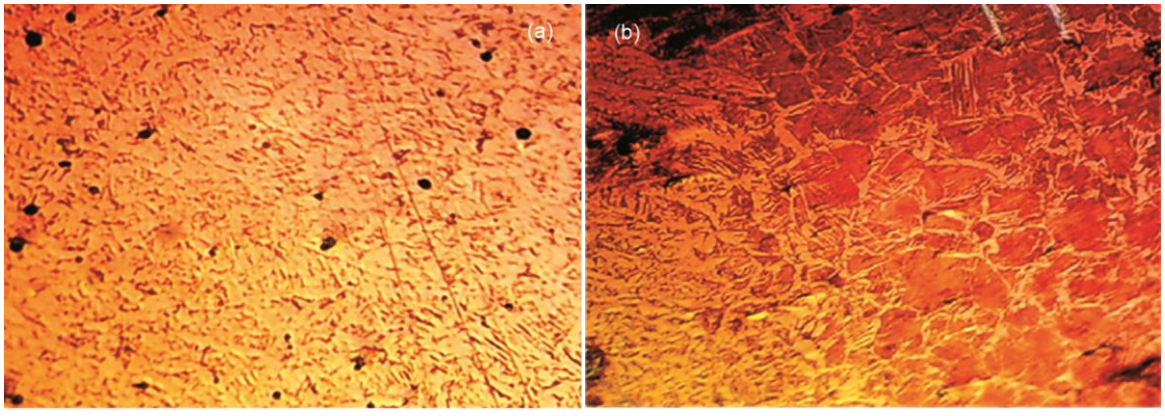

Fig. 6 — Microstructure of weld sample no. 1 (a) weld zone, and (b) fusion boundary.

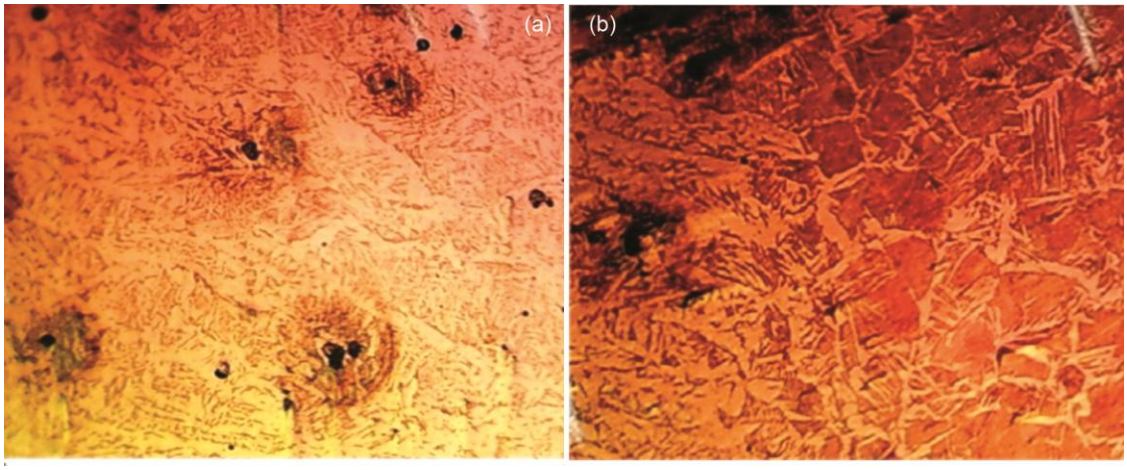

Fig. 7 — Microstructure of weld sample no. 2 (a) weld zone, and (b) fusion boundry.

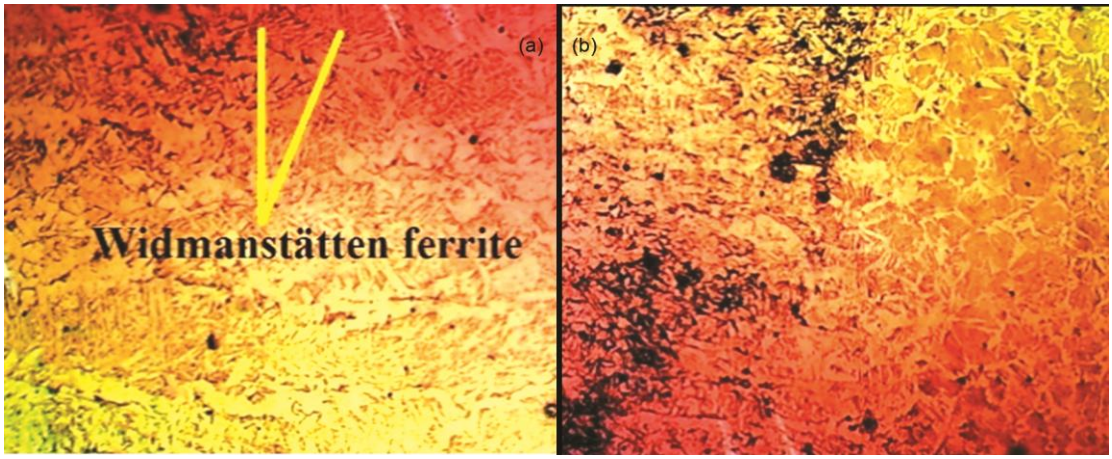

Fig. 8 — Microstructure of weld sample no. 4 (a) weld zone, and (b) fusion boundary.

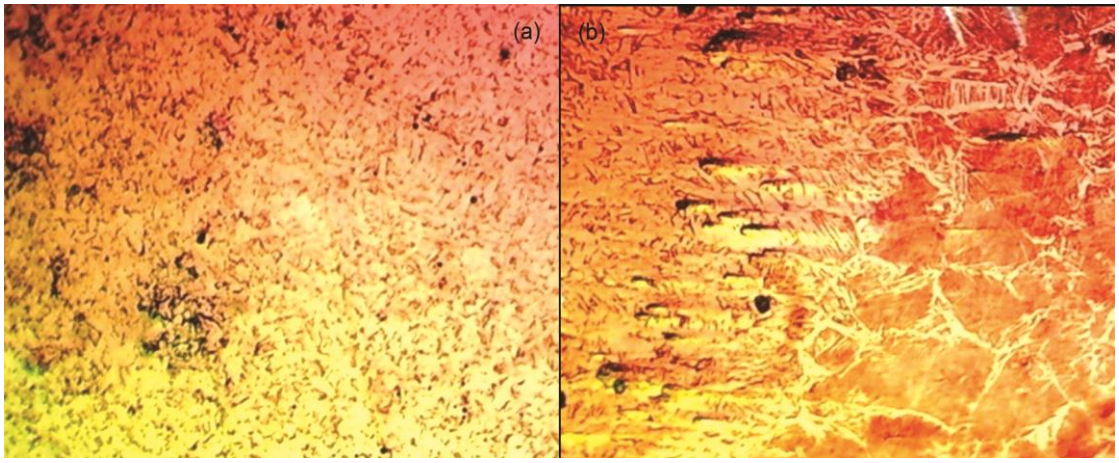

Fig. 9 — Microstructure of weld sample no. 6 (a) weld zone, and (b) fusion boundary.

and the actual size of dendrites also increases. This may be because of increases in heat input energy which in turn reduces cooling rate[24] which results in a decrease in hardness and increase in impact strength of weldment. Thus it was observed that the microstructure is the clear image of the welded sample. The boundaries of all different zones can be analyzed with microstructural analysis.

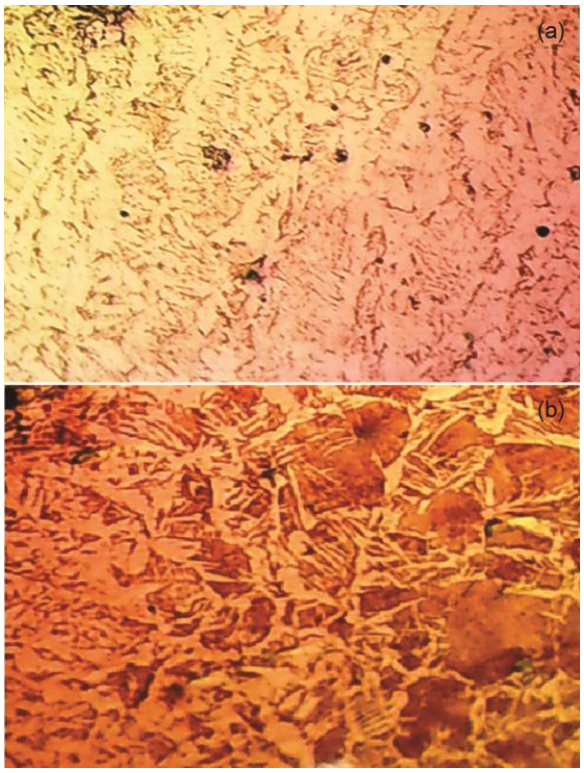

Fig. 10 — Microstructure of weld sample no. 8 (a) weld zone, and (b) fusion boundary.

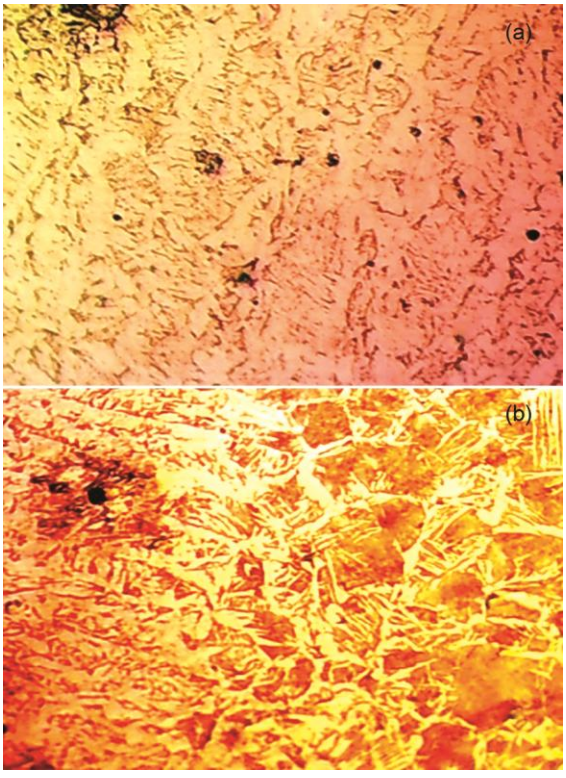

Fig. 11 — Microstructure of weld sample no. 9 (a) weld zone, and (b) fusion boundary.

4 Conclusion

The following conclusions may be derived from the present experimental investigations:

- On increasing the heat input absorbed energy (toughness) value increased while Ultimate Tensile Strength (UTS) decreased.
- The Microhardness of welded joints in transverse and lateral direction decreases with an increase in toughness (energy).
- On increasing the heat input value there is an increment in the grain size of weldment, this leads to an increase in ductility and toughness.
- From fractography of welded joints,the ductile fracture was observed with large numbers of dimples.
- From microstructure investigation of weldments it was observed that on increasing the heat input value, there is an increment in grain size of weldments. This leads to an increase in ductility and toughness.
- Increasing the heat input value led to grain growth in the weldment zone and results in the tempering of the martensitic structure.

References

1 Dhua, S K, Mukerjee D, & Sarma D S, *ISIJ International*, 42(2002) 290.
2 Xue Q, Benson D, Meyers M A, Nesterenko V F, & Olevsky E A, *Mater Sci Eng A*, 354(2003)166.
3 Jorge, J C F, Monteiro, J L D, Gomes A J D C, Bott I D S, Souza L F G De, Mendes M C, & Araújo LS, *J Mater Res Technol*, 8(2019) 561.
4 M M Arif, Shrikrishna K A, Sathiya P, & Goel S, *J Manuf Process*, 18(2015) 92.
5 Grajcar A, Różański M, Stano S, & Kowalski A, *J Mater Eng Perform*, 23(2014) 3400.
6 Wen C, Wang Z, Deng X, Wang G, & Misra R D K, *Steel Res Int*, 89 (2018) 1700500.
7 Li H L, Liu D, Yan Y T, Guo N, Liu Y B, & Feng J C, *J Manuf Process*, 31(2018) 833.
8 Murti V S R, Srinivas P D, Banadeki G H D, & Raju K S, *J Mater Process Technol*, 37(1993)723.
9 Nagesh D S, & Datta G L, *Appl Soft Comput*, 10(2010) 897.
10 Padmanaban M R A, Baskar N, & Kandasamy D, *Mater*, 20(2017) 76.
11 Kumar V, Hussain M, Singh R, & Kumar S, *Adv Sci Eng Med*, 12(2020)888.
12 Kumar S, Singh R, Jaiswal R, & Kumar A, *Int J Eng Trans B Appl*, 33(2020)870
13 Singh R, Rizvi S A, Saxena K K, &. Godara S S, *Adv Mater Process* (2021)1.
14 Rizvi S A, *IJE TRANSACTIONS C: Aspects* 33(2020)1811.
15 Jorge J C F, de Souza L F G, Mendes M C, Bott I S, Arau´ jo L S, dos Santos V R, Rebello J M A, & Evans G M, *J Mater Res Technol* 10 (2021) 471.
16 Keshav P, & Dwivedi D K, *Mater Manuf Process*, 23: (2008) 463.

17 Nathan S R, Balasubramanian V, Malarvizhi S, & Rao A G, *Def Technol*, 11 (2015) 308.
18 Chena L, Niea P, Qub Z, Ojoc O A, Xiab L, Lia Z, & Huang J, *J Manuf Process*, 50(2020) 132
19 Francois N B, Paul K, Pavel L, & Victor K, *Metals* 9 (2019) 355.
20 Adam G, Maciej R, Sebastian S, Aleksander K, & Barbara G, *Adv Mater Sci Eng*, (2014) 1.
21 Ribeiro H V, Baptista C A R P , Lima M S F , Torres M A S, & Marcomini J B, *J Mater Res Technol*, 11 (2021) 801.
22 Qin H, Tang Y, & Liang P, *Int J Electrochem Sci*, 16 (2021) 210449.
23 Zhang J, Xin W , Luo G, Wang R, & Meng Q, *High Temp Mater Proc*, 39 (2020) 33.
24 Bayock F N, Kah P, Layus P, & Karkhin V, *Metals* 9 (2019) 355.